Real time feedback on plasma radiation at W7-X

P.Hacker[1, 2], F.Reimold[1], D.Zhang[1]

[1]Max-Planck-Institute for Plasmaphysics, Wendelsteinstr. 1, Greifswald, Germany

[2]University of Greifswald, Rubenowstr. 6, Greifswald, Germany

25th of Sept., 2020

This work has been carried out within the framework of the EUROfusion Consortium and has received funding from the Euratom research and training programme 2014-2018 under grant agreement No 633053. The views and opinions expressed herein do not necessarily reflect those of the European Commission.

Contents

Bolometer

What is the Bolometer at W7-X?

– two camera system using metal film resistive detector arrays to measure plasma radiation based on thermal effects

⇒ measure global & local power balance, investigation of radiation power loss, mainly from impurities, and its distribution

HBCm

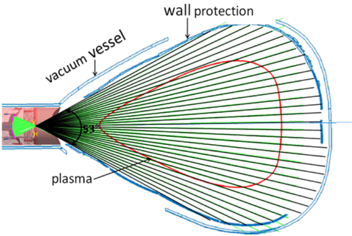

VBCr/VBCl

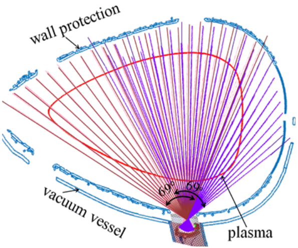

(Lines of sight with individual apertures, retracted into the vacuum vessel, D.Zhang et al.)

Plasma Radiation

$$P_{rad} \propto \sum_Z n_e \cdot n_Z \cdot L_Z$$

> L_Z: total radiation coefficient, incl. line & continuum radiation of impurity Z
> $\ldots = f\left(T_e,\ T_i,\ T_Z,\ wall\ material/conditions,\ \ldots\right)$

Plasma Radiation

$$P_{rad} \propto \sum_Z n_e \cdot n_Z \cdot L_Z$$

$$P_{rad,bolo} = \frac{V_{P,tor}}{V_{cam}} \cdot \sum_{ch} \frac{P_{ch} \cdot V_{ch}}{K_{ch}}$$

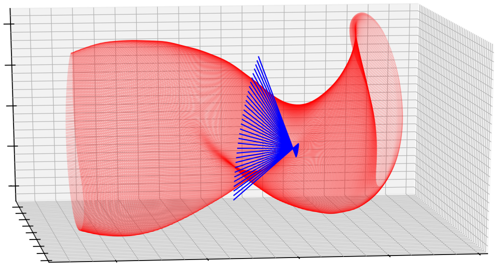

(LoS of HBCm in 90° subsection of magnetic standard configuration fluxsurfaces; P. Hacker et al)

Calculations

Plasma Radiation

$$P_{rad} \propto \sum_{Z} n_e \cdot n_Z \cdot L_Z$$

$$P_{rad,bolo} = \frac{V_{P,tor}}{V_{cam}} \cdot \sum_{ch} \frac{P_{ch} \cdot V_{ch}}{K_{ch}}$$

Bolometer equation:

$$P_{ch} = F_{ch} \cdot \left(\Delta U + f_{\tau,ch} \frac{\mathrm{d}(\Delta U)}{\mathrm{d}t} \right)$$

> $\Delta U \propto \Delta T$ the change in absorber temperature

> $f_{\tau,ch}$ cooling factor of detector

Feedback: Goals

Goal

Providing feedback signal for *fast feedback gas valve* diagnostic through fast (5 ms) calculation of P_{rad} estimate

Investigations

1.- adjust divertor heat loads, investigate radiation regimes, dedicated detachment

2.- find relationship between gas puff and radiation power loss for both intrinsic and extrinsic impurities

Prediction

> fast radiation power proxy for subset S of channel selection:

$$P_{pred} = f \cdot \frac{V_{P,tor}}{V_S} \sum_S \frac{V_{ch} \cdot P_{ch}}{K_{ch}}$$

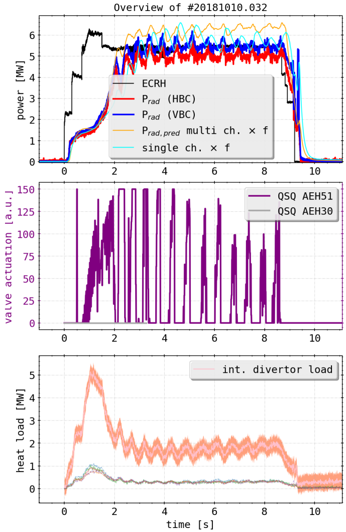

(Overview plot, P_{rad}, P_{pred}, valve actuation and integrated divertor target heat load; P.Hacker et al.)

Feedback: Sensitivity

Problem

What subset of channels and/or cameras S yields the best prediction and feedback performance?

Response

- $>$ subset S of 3 - 7 channels with LoS both tangential to *scrape-off layer* (SOL) and through core
- $>$ no more than a selection of 9 possible $\Rightarrow$ calculation too slow

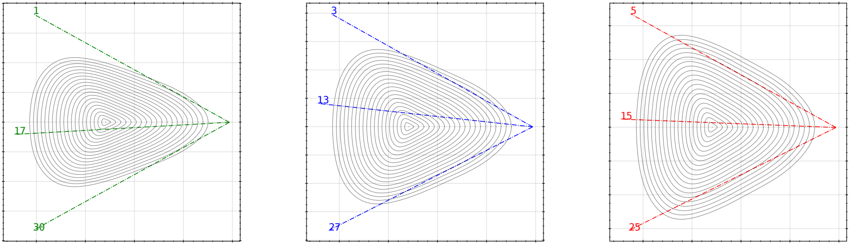

Examples of LoS selections S from HBCm (P.Hacker et al.)

Feedback: Sensitivity

Prediction Quality Metric

- prediction from set S using Bolometer equation $P_{pred,S}$ to define a weighted, normalised cost function:

<u>deviation:</u> $$d_S = \left\| P_{rad,cam}(t) - P_{pred,S}(t) \right\|$$

<u>weighted:</u> $$\varepsilon_S(t) = \left\{ \begin{array}{ll} 1 - \frac{d_S(t)}{P_{rad}(t)} & , \; d_S(t) < P_{rad}(t) \\ 0 & , \; \text{else} \end{array} \right\}$$

<u>quality:</u> $$\vartheta_S = \int_T \varepsilon_S(t) \mathrm{d}t$$

- e.g. $\varepsilon_{HBC}(t) = 1$ and consequently $\vartheta_{HBC} = 1$

Prediction Quality Metric

weighted: $$\varepsilon_S(t) = \begin{cases} 1 - \frac{d_S(t)}{P_{rad}(t)} & , \; d_S(t) < P_{rad}(t) \\ 0 & , \; \text{else} \end{cases}$$

quality: $$\vartheta_S = \int_T \varepsilon_S(t) \mathrm{d}t$$

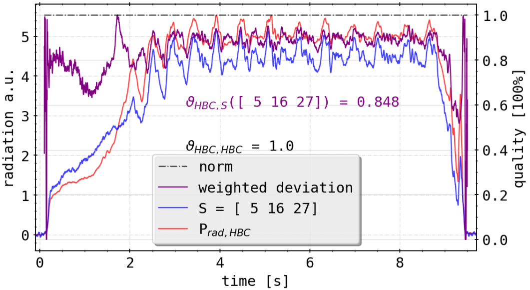

(XP: 20181010.032, P_{rad}, P_{pred} and cost function for one subset of channels with $n = 3$; P.Hacker et al.)

Statistics: Example

- > pre-selecting combinatory space for subsets, i.e. only LoS from SOL and core regions
- > N_n the total number of tested channel subsets S_n with prediction consisting of n individual LoS

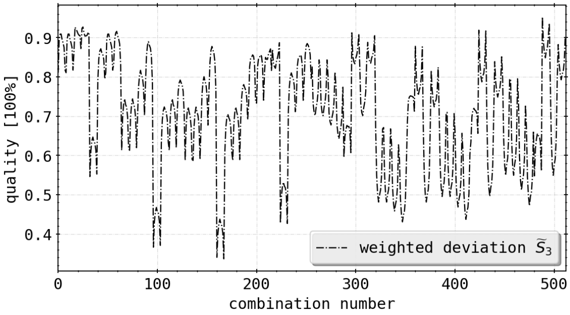

(XP: 20181010.032, P_{rad}, P_{pred} and cost function for one subset of channels with $n = 3$; P.Hacker et al.)

Feedback: Statistics

Statistics: Example

- pre-selecting combinatory space for subsets, i.e. only LoS from SOL and core regions
- N_n the total number of tested channel subsets S_n with prediction consisting of n individual LoS
- be N_{ch}^n the amount of subsets S_n that include channel/LoS ch

  total sensitivity:

$$\Omega_{ch}^n = \frac{1}{N_{ch}^n} \sum_{S_{ch}}^{N} \vartheta_{HBC,S^{ch}}$$

Statistics: Example

total sensitivity:

$$\Omega_{ch}^{n} = \frac{1}{N_{ch}^{n}} \sum_{S_{ch}}^{N} \vartheta_{HBC,S^{ch}}$$

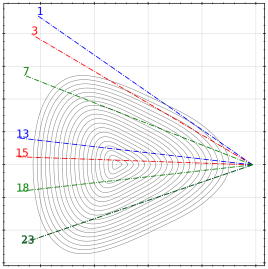

(Selections S including $\#$ 23)

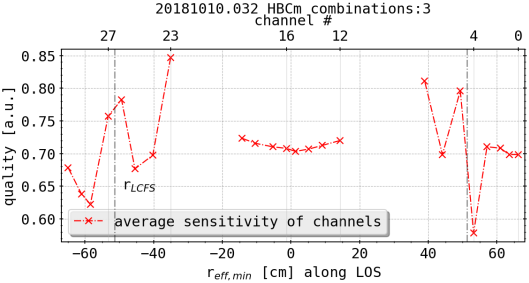

(XP: 20181010.032, Ω^{3}_{ch}; P.Hacker et al.)

Statistics: Example

- base quality of channel combinations $\approx 60\%$ from educated pre-selection
- total sensitivity at minimum 60% for individual contributions from LoS to predictions

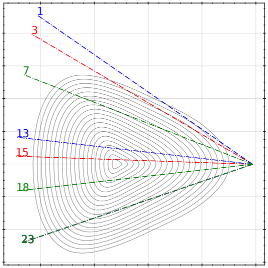

(Selections S including $\#$ 23)

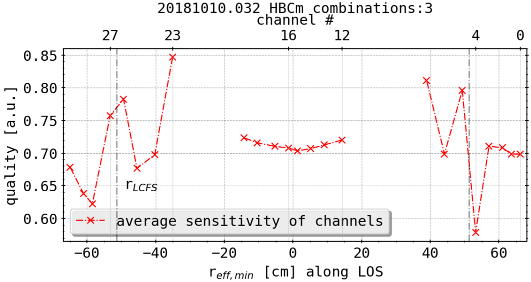

(XP: 20181010.032, Ω^3_{ch}; P.Hacker et al.)

Statistics: Example

- $>$ maximum sensitivity around SOL or *last closed fluxsurface*
- $>$ combination of *best* channels in one subset can achieve up to $\vartheta_S \approx 0.95$ without any further proportionality factors

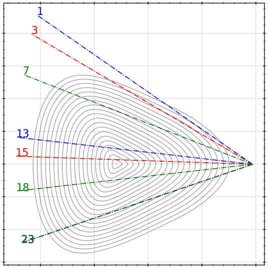

(Selections S including # 23)

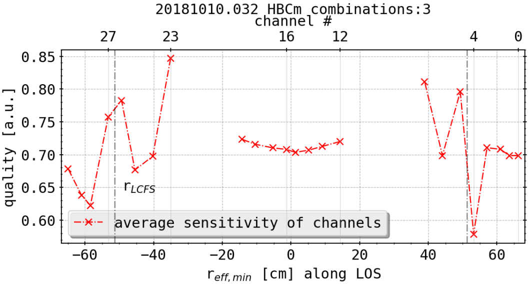

(XP: 20181010.032, Ω^3_{ch}; P.Hacker et al.)

Consequences: Radiation Fraction

- feedback controlled experiment reaches target of $f_{rad} = P_{rad}/P_{ECRH} \approx 1.0$ when seeded by fast feedback gas valve
- increasing radiation power loss until cycling between $f_{rad} \sim 0.9$ & 1.0

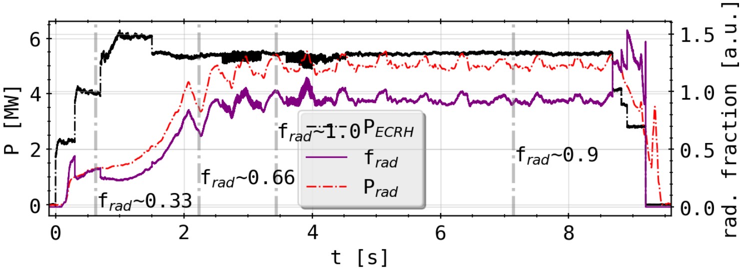

(XP: 20181010.032; P.Hacker et al.)

Consequences: Radiation Fraction

- line-integrated chordal profile shows majority of radiation coming from region close to separatrix or SOL
- increasing radiation fraction shows inward shift of brightness away from last closed fluxsurface ⇒ Why?

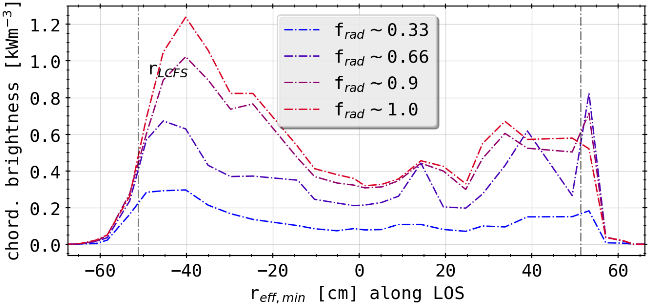

(XP: 20181010.032, chordal brightness (i.e. power density) of HBCm at fix radiation fractions; P.Hacker et al.)

Intrinsic Impurities: STRAHL Results

> suspecting intrinsic impurity C ionisation to be very sensitive to separatrix electron temperature & density

> calculating radial transport $\Gamma_{i,Z}$ and emission of impurity i and ion-stage Z solving continuity equation using ansatz of anomalous diffusivities D^* and radial drift velocities v^*:

$$\begin{aligned}\frac{\partial n_{i,Z}}{\partial t} &= -\nabla \Gamma_{i,Z} + Q_{i,Z} \\ &= \frac{1}{r}\frac{\partial}{\partial r} r \left(D^* \frac{\partial n_{i,Z}}{\partial r} - v^* n_{i,Z} \right) + Q_{i,Z}\end{aligned}$$

Intrinsic Impurities: STRAHL Results

> radial line radiation profiles for C^{X+} ions in coronal equilibrium for $f_{rad} = 0.9$ and 1.0 experience inward shift

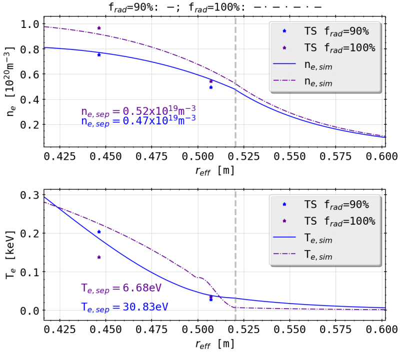

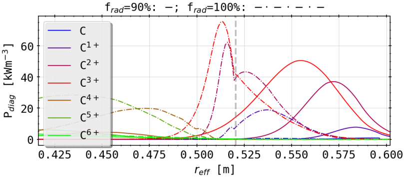

(Input profiles and ionization radiation for C^{X+} calculated by STRAHL for $f_{rad} \in [0.9,\ 1.0]$; P.Hacker et al.)

Method: Mimimum Fischer Regularization

general problem: $$T * g = f_m$$

regularization: $$\underset{g}{\text{argmin}} \left[(T * g - f_m)^2 + \lambda \mathcal{R} \right]$$

> T: LoS geometry information on inversion grid
> f_m: line intgrated power for each channel
> g: matrix containing radiation per channel & pixel
> $\lambda \in \mathbb{R}$: regularization parameter
> $\mathcal{R}$: regularization functional, constraint to solution

Method: Mimimum Fischer Regularization

general problem: $$T * g = f_m$$

regularization: $$\underset{g}{\operatorname{argmin}} \left[(T * g - f_m)^2 + \lambda \mathcal{R} \right]$$

Fisher regularization: $$\underset{g}{\operatorname{solve}} \left(T^{\intercal} T + \lambda \mathcal{H}^{(n)} \right) * g^{(n+1)} = T^{\intercal} * f_m$$

$$\mathcal{H}^{(n)} = \nabla_x^{\intercal} * W^{(n)} * \nabla_x + \nabla_y^{\intercal} * W^{(n)} * \nabla_y$$

> $(\cdot)^{(n)}$: iterative process to find *argmin*

> $W^{(n)}$: *gradient based* weighting matrix

Tomography: STRAHL Results

$f_{rad} \sim 0.33$

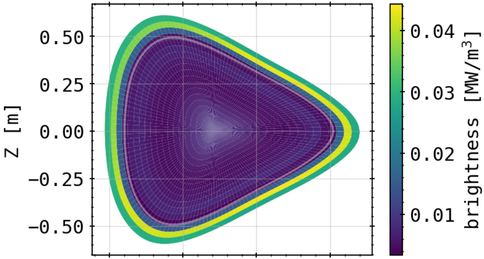

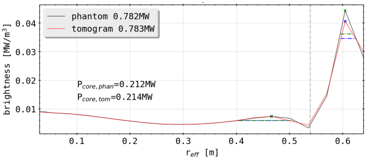

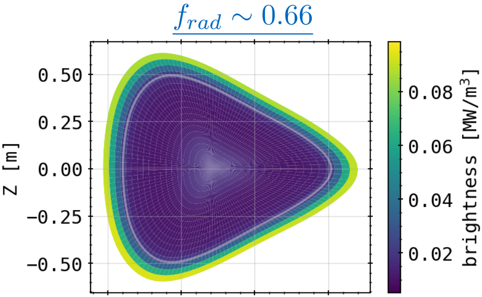

$f_{rad} \sim 0.66$
0.50
0.25
0.00
−0.25
−0.50
Z [m]
0.08
0.06
0.04
0.02
brightness [MW/m^3]

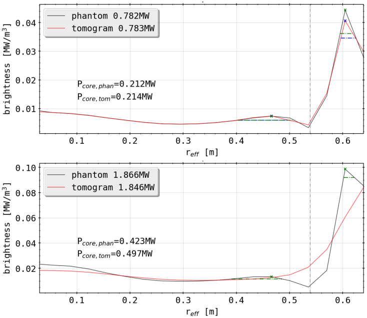

phantom 0.782MW
tomogram 0.783MW
$P_{core,phan}$=0.212MW
$P_{core,tom}$=0.214MW
brightness [MW/m^3]
r_{eff} [m]
phantom 1.866MW
tomogram 1.846MW
$P_{core,phan}$=0.423MW
$P_{core,tom}$=0.497MW
brightness [MW/m^3]
r_{eff} [m]

Tomography: STRAHL Results

$f_{rad} \sim 0.9$

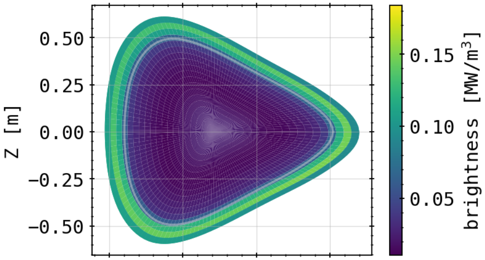

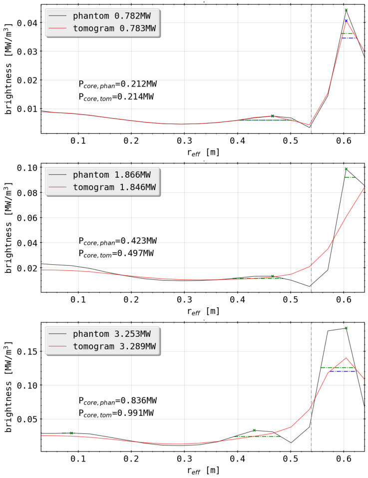

Tomography: STRAHL Results

$f_{rad} \sim 1.0$

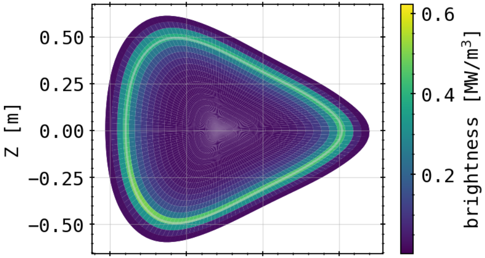

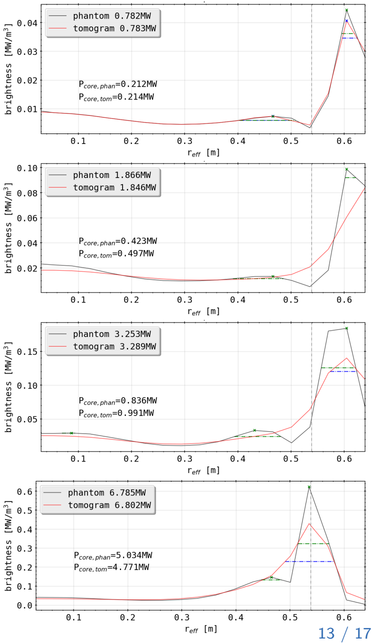

$f_{rad} \sim 0.33$

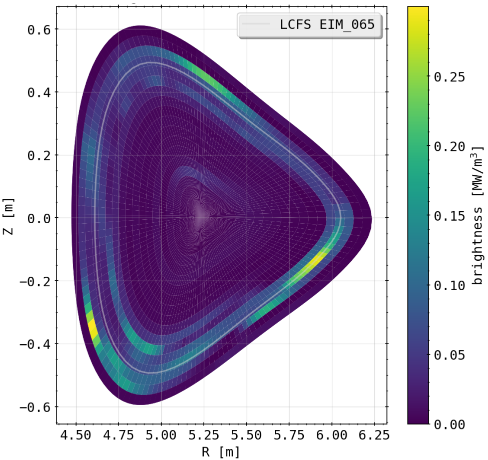

LCFS EIM_065
Z [m]
R [m]
0.6
0.4
0.2
0.0
−0.2
−0.4
−0.6
4.50
4.75
5.00
5.25
5.50
5.75
6.00
6.25
brightness [MW/m3]
0.25
0.20
0.15
0.10
0.05
0.00

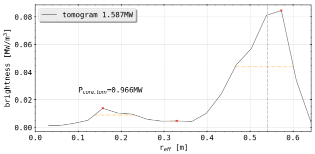

tomogram 1.587MW
P core, tom=0.966MW
brightness [MW/m3]
r eff [m]
0.08
0.06
0.04
0.02
0.00
0.0
0.1
0.2
0.3
0.4
0.5
0.6

$f_{rad} \sim 0.66$

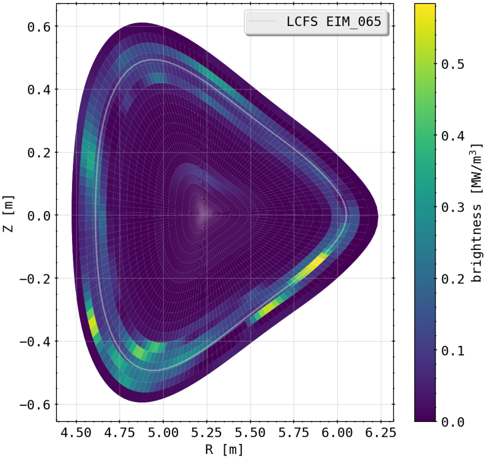
LCFS EIM_065
Z [m]
R [m]
brightness [MW/m³]

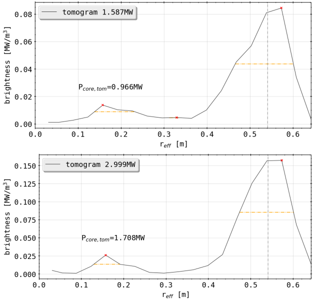
tomogram 1.587MW
P_core, tom=0.966MW
brightness [MW/m³]
r_eff [m]
tomogram 2.999MW
P_core, tom=1.708MW
brightness [MW/m³]
r_eff [m]

$f_{rad} \sim 0.9$

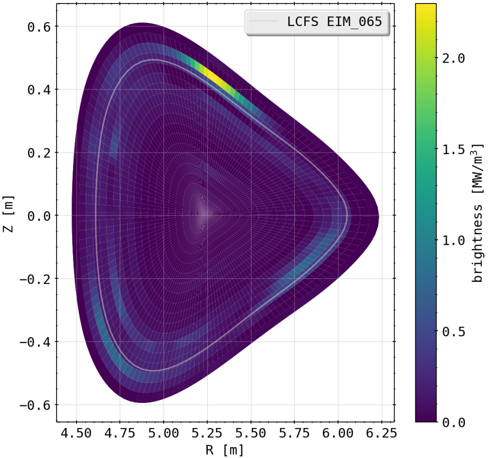
LCFS EIM_065
Z [m]
R [m]
brightness [MW/m^3]

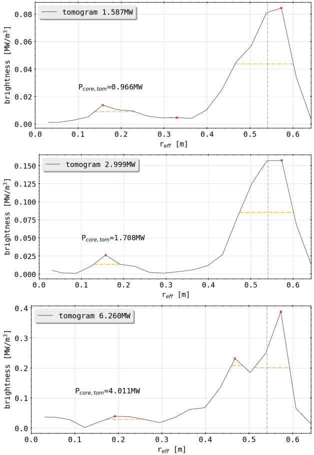
tomogram 1.587MW
P$_{core,tom}$=0.966MW
tomogram 2.999MW
P$_{core,tom}$=1.708MW
tomogram 6.260MW
P$_{core,tom}$=4.011MW
brightness [MW/m^3]
r$_{eff}$ [m]

Tomography: Experiment 20181010.032

$f_{rad} \sim 1.0$

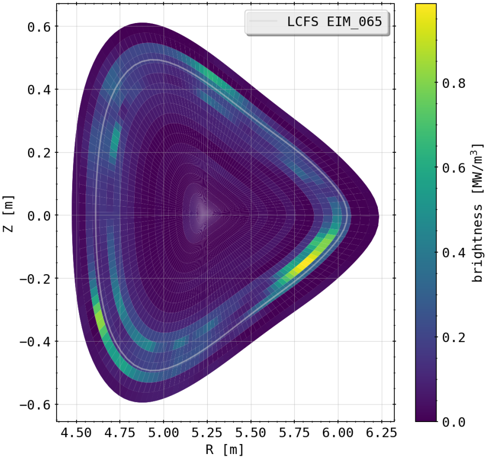

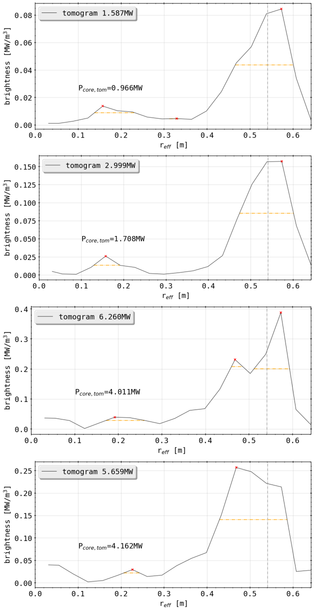

Conclusions

Sensitivity Study

- benchmarks on different experiments, cost metrics and camera/channels subsets (up to $n = 9$) show similar results
- Bolometer most sensitive to changes in radiation distribution along separatrix and SOL

Simulation and Inversion

- STRAHL shows strong radial dependence of intrinsic impurity radiation regarding separatrix electron temperature and density
- C^{X+} radiation close to seperatrix indicator for regimes of detachment
- need 2D inversion of radiation distribution to validate results and to understand profiles

Thank you for your attention!

Bibliography

- "Design Criteria of the Bolometer diagnostic for steady-state operation of the W7-X stellarator"; Zhang, D. et al.; Review of Scientific Instruments, Jan 1st, 2010; DOI:10.1063/1.3483194
- "The bolometer diagnostic at stellarator Wendelstein 7-X and its first results in the initial campaign"; D. Zhang, et al. and the W7-X Team; Stellarator-New 2017
- "A low noise highly integrated bolometer array for absolute measurement of VUV and soft x radiation"; K. F. Mast et. al; Review of Scientific Instruments 62, 744 (1991); DOI: 10.1063/1.11.42078
- "Steepest descent moment method for three dimensional magnetohydrodynamic equilibria"; Hirshman, S.P. et al.; Physics of Fluids 26, 3553, (1983); DOI: 10.1063/1.864116
- "Tokamaks"; Wesson, J.; Clarendon Press, Oxford; 1987

Bibliography

- "Numerical investigation of plasma edge transport and limiter heat fluxes in Wendelstein 7-X startup plasmas with EMC3-EIRENE"; Effenberg, F., Feng, Y. et al. Nucl. Fusion 57 (2017) 036021 (15pp); DOI: 10.1088/1741-4326/aa4f83
- "Derivation of bolometer equations relevant to operation in fusion experiments"; Gianone, L. et al.; Review of Scientific Instruments; 20th of November, 2002; DOI: 10.1063/1.1498906
- "Results of the bolometer diagnostic at OP 1.a of W7-X"; internal review of the physics plan during the second operational phase at the stellarator W7-X; 28.02.20i18
- "Characterization of energy confinement in net-current free plasmas using the extended International Stellarator Database"; H. Yamada et al.; INSTITUTE OF PHYSICS PUBLISHING and INTERNATIONAL ATOMIC ENERGY AGENCY; Nucl. Fusion 45 (2005) 1684¿1693
- "Introduction to the Queue Data Structure – Array Implementation"; URL: https://www.thecodingdelight.com/queue-data-structure-array-implementation/